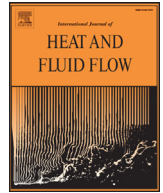




Contents lists available at ScienceDirect

International Journal of Heat and Fluid Flow

journal homepage: www.elsevier.com/locate/ijhff

Analysis of dimensionality effect on shock wave boundary layer interaction in laminar hypersonic flows

Bibin John^a, Srikanth Surendranath^b, Ganesh Natarajan^b, Vinayak Kulkarni^{b,*}

^aSchool of Mechanical Engineering, VIT University, Vellore, 632 014 India

^bDepartment of Mechanical Engineering, IIT Guwahati, Guwahati, 781 039 India

ARTICLE INFO

Article history:
Available online xxx

Keywords:
Shock wave boundary layer interactions
Laminar flow
Hypersonics
Bluntness
Flow separation

ABSTRACT

Present investigations are centered on passive control of shock wave boundary layer interaction (SWBLI) for double cone and double wedge configurations with leading edge bluntness. This study seeks the differences in the flow physics of SWBLI in case of two dimensional (2D) and axisymmetric flow fields. In-house developed second order accurate finite-volume 2D axisymmetric compressible flow solver is employed for these studies. It is observed that the idea of leading edge bluntness offers reduction in separation bubble for 2D flow fields, whereas it leads to enhanced separation zone in case of axisymmetric flow fields. Relevant flow physics is well explored herein using wall pressure profile and relative thicknesses of boundary layer and entropy layer. Thicker entropy layer and stronger favorable pressure gradient are found responsible for the possibility of separation control in case of 2D flow fields. Thin entropy layer due to three dimensional relieving effect and its swallowing by the boundary layer are attributed for higher separation bubble size in case of cone with range of radii under consideration.

© 2016 Elsevier Inc. All rights reserved.

1. Introduction

Shock wave boundary layer interaction (SWBLI) is the classical example of flow field complexity in the field of compressible flow aerodynamics. Such interactions are often seen with impingement of shock on the boundary layer or in case of sudden turning of the flow around compression corners. The former can be termed as impingement based shock wave boundary layer interaction (I-SWBLI) while the later can be named as ramp induced shock wave boundary layer interaction (R-SWBLI). Double cone or double wedge geometries are preferred for understanding of R-SWBLI. Shock generators or variable area ducts are generally employed for I-SWBLI studies. Such simple configurations help in simulating and understanding the flow pattern around complex configurations like engine inlet, wing-body junction, control surfaces etc. These vehicle components or subsystems invariably encounter SWBLI where intensity of interaction depends upon the flow deflection angle. At lesser or greater extent, this phenomenon is responsible for limiting the aircraft performance, structural damage and degradation of engine efficiency due to possibility of separation. Hence understanding of this flow feature is essential to avoid, delay or control the interaction. In view of this, R-SWBLI

(Needham and Stollery, 1966; Holden, 1978; Marini, 1998; John and Kulkarni, 2014a; John et al., 2014) and I-SWBLI (Vito et al., 2014; Laura and John, 2015) have been investigated to access and to comprehend the influence of geometric and flow properties on the interaction. It can be depicted from those findings that the strength of interaction increases with decrease in freestream stagnation enthalpy, freestream Mach number, wall temperature and increase in ramp angle. Similar studies on SWBLI over axisymmetric geometries are also reported by few researchers (Dieudonne et al., 1999; Savino and Paterna, 2005).

Intense shock wave boundary layer interaction may lead to increased surface heating (John et al., 2014), vortex shedding, broadband noise (Pirozzoli and Grasso, 2006) and transition to turbulence (Dietz and Hein, 1999). Consequently, implementation of preventive or control measures is highly desirable to reduce the intensity of this interaction. Passive technique like provision of leading edge bluntness (Coët and Chanetz, 1993; Holden, 1970; Holden, 1971; Neuenhahn and Olivier, 2009; John and Kulkarni, 2014b) and active techniques like boundary layer suction and blowing or cooling (Lewis et al., 1968; Schulte et al., 2001) are considered to suppress the this undesirable interaction. However, provision of the leading edge bluntness is a simple mechanism to implement passive separation control technique. Experimental investigation of Coët et al. (Coët and Chanetz, 1993) favors this technique for its practical implementation. However, some researchers have noticed that initial increment in leading edge radius increases

* Corresponding author. Fax: +91 361 2690762.
E-mail address: vinayak@iitg.ernet.in (V. Kulkarni).

Nomenclature

ρ	Density
μ	Coefficient of dynamic viscosity
α	Constant about dimensionality
τ	Shear stress
C_f	Skin friction coefficient
C_p	Pressure Coefficient
E_l	x-component of inviscid flux vector
F_l	y-component of inviscid flux vector
E_v	x-component of viscous flux vector
F_v	y-component of viscous flux vector
H	Total Enthalpy
L_b	Separation bubble size
M	Mach number
P	Pressure
q	Heatflux
Re	Reynolds Number
R_n	Leading edge radius
t	time
T	Temperature
U	Conservative variable vector
u	Velocity in x-direction
v	Velocity in y-direction
x,y,z	Axes of co-ordinate system

Subscripts

∞	Free stream conditions
w	Wall properties

the separation size which attains a peak at the critical radius (inversion radius) (Holden, 1970; Neuenhahn and Olivier, 2009). Reasoning of this separation dynamics till this critical radius, given by those researchers, is based on two distinct observations. Albeit, the unified interpretation points to the fact that lesser thickness of entropy layer in comparison with the boundary layer is responsible for separation zone widening (Neuenhahn and Olivier, 2009; John and Kulkarni, 2014b). Beyond the first critical or inversion radius, separation region shrinks in size with increment in leading edge bluntness. In this process, a critical radius (equivalent radius) is encountered above which decrement in separation bubble size, in comparison with the sharp leading edge geometry, will be assured. Therefore, it is essential to know the value of second critical or equivalent radius for effective separation control. However most of such findings are concerned with the two dimensional (2D) flow field only. In view of this, present studies focus on flow field alterations in the presence of leading edge bluntness for separation control in case of axi-symmetric flows. These investigations are thus based on identification of the critical radii for two dimensional and axi-symmetric flow fields and understanding the flow physics at those radii. Such studies are essential to analyze the dimensionality effect on the magnitudes of critical radii (inversion radius and equivalent radius) for given flow turning angle, freestream conditions and wall boundary conditions. Present findings would also reveal the possible reasons for change in magnitudes of critical radii with change in dimensionality and would provide associated cautious remark. For the present motivations, necessary computations are carried out using an in-house CFD solver (John and Kulkarni, 2014a; John et al., 2014; John and Kulkarni, 2014b) while the freestream conditions and geometry are taken from the literature (Dieudonne et al., 1999). Details about the solver, test conditions and results are given in following sections.

2. Numerical methodology

The present numerical investigations for two dimensional and axisymmetric flowfields are carried out with an in-house developed unstructured compressible laminar flow solver. This in-house solver, USHAS (John and Kulkarni, 2014a; John et al., 2014; John and Kulkarni, 2014b) (Unstructured Solver for Hypersonic Aerothermodynamic Simulations), considers 2D-axisymmetric Navier Stokes equations given by,

$$\frac{\partial U}{\partial t} + \frac{\partial E_l}{\partial x} + \frac{\partial F_l}{\partial y} + \alpha H_l = \frac{\partial E_v}{\partial x} + \frac{\partial F_v}{\partial y} + \alpha H_v \quad (1)$$

where, U is the conservative variable vector, E_l and F_l are the convective flux vectors in x and y directions respectively. Similarly E_v and F_v are the corresponding x and y -directional viscous flux vectors. Here, H_l and H_v are inviscid and viscous source terms respectively. All these vectors from Eq. (1) are given by,

$$U = \begin{bmatrix} \rho \\ \rho u \\ \rho v \\ \rho E \end{bmatrix} \quad E_l = \begin{bmatrix} \rho u \\ \rho u^2 + p \\ \rho uv \\ \rho uH \end{bmatrix} \quad F_l = \begin{bmatrix} \rho v \\ \rho uv \\ \rho v^2 + p \\ \rho vH \end{bmatrix}$$

$$E_v = \begin{bmatrix} 0 \\ \tau_{xxp} \\ \tau_{xy} \\ u\tau_{xxp} + v\tau_{xy} - q_x \end{bmatrix} \quad F_v = \begin{bmatrix} 0 \\ \tau_{xy} \\ \tau_{yyp} \\ u\tau_{xy} + v\tau_{yyp} - q_y \end{bmatrix}$$

$$H_l = \frac{1}{y} \begin{bmatrix} \rho v \\ \rho uv \\ \rho v^2 \\ (\rho E + p)v \end{bmatrix}$$

$$H_v = \frac{1}{y} \begin{bmatrix} 0 \\ \tau_{xy} - \frac{2}{3} \frac{y}{Re_\infty} \frac{\partial(\mu v/y)}{\partial x} \\ \tau_{yyp} - \tau_{\theta\theta} - \frac{2}{3} \frac{\mu}{Re_\infty} \left(\frac{v}{y}\right) - \frac{y}{Re_\infty} \frac{2}{3} \frac{\partial(\mu v/y)}{\partial y} \\ u\tau_{xy} + v\tau_{yyp} - q_y - \frac{2}{3} \frac{\mu}{Re_\infty} \frac{v^2}{y} - \frac{y}{Re_\infty} \frac{2}{3} \frac{\partial(\mu v^2/y)}{\partial y} - \frac{2}{3} \frac{y}{Re_\infty} \frac{\partial(\mu uv/y)}{\partial x} \end{bmatrix} \quad (2)$$

Here α is unity for axi-symmetric flows and is zero for 2D flows. Non-dimensional form of these equations is considered while developing the present solver. Freestream conditions and the plate length upstream of the ramp are considered as reference parameters for non-dimensionalisation of various terms in above equation.

Algorithm of USHAS is capable to handle the unstructured data structure. This feature of the solver enables it to consider various mesh topologies. Second order accuracy has been ensured herein for spatial discretisation through the use of piecewise linear reconstruction method. Although the solver holds the provision of seven convective flux calculation methodologies, AUSM+ has been considered for present studies due to its comparative advantages for high speed flow simulations. Viscous fluxes are obtained directly using the cell centroid gradient which is calculated by means of discrete version of Green-Gauss theorem. Implicit time stepping is incorporated to accelerate the convergence (Ganesh et al., 2009).

3. Results and discussion

3.1. Mesh independence study and solver validation

Validation of the solver and grid independence study are initially performed for the test case of Mach 6 flow over a blunted cone flare configuration at zero degree angle of incidence. Experimental results for this axi-symmetric case are available in the open literature (Dieudonne et al., 1999). These experiments were carried

Download English Version:

<https://daneshyari.com/en/article/4993241>

Download Persian Version:

<https://daneshyari.com/article/4993241>

[Daneshyari.com](https://daneshyari.com)